Theory of anomalous proximity effects in phase-coherent structures

N. R. Claughton
School of Physics and Materials, Lancaster University, Lancaster LA1 4YB, United Kingdom

V. C. Hui
D.R.A., Electronics Division, Malvern, Worcester WR14 3PS, United Kingdom

C. J. Lambert
School of Physics and Materials, Lancaster University, Lancaster LA1 4YB, United Kingdom
(Received 4 August 1994; revised manuscript received 28 October 1994)

We present theoretical results for the change δG in the electrical conductance G of a mesoscopic sample due to the switching on of superconductivity. Due to competition between normal and Andreev scattering, the sign of δG depends in detail on the impurity configuration within a device. In contrast with universal conductance fluctuations, we demonstrate that δG can scale with the system size and therefore, as well as being negative, can have a magnitude much greater than $2e^2/h$. For clean systems, this anomalous behavior arises from low-angle quasiparticle scattering at normal-superconducting interfaces. For dirty systems it arises from the presence of normal-state conductance resonances. We also examine the magnetic-field dependence of δG and show that fields on the scale of a flux quantum through a sample can change the sign of δG and suppress its magnitude. For a superconducting order parameter of magnitude Δ_0, we present results for the Δ susceptibility $\chi_\Delta = \lim_{\Delta_0 \to 0} \partial G(\Delta_0)/\partial \Delta_0^2$. For clean systems, where the normal-state conductance is quantized in units of $2e^2/h$, we predict that χ_Δ diverges at normal-state conductance steps. For dirty systems, it is shown that χ_Δ is sensitive to the local environment of single impurity atoms.

I. INTRODUCTION

While the separate fields of superconductivity and normal-state mesoscopic physics are now relatively mature, the subject of mesoscopic superconductivity is a new area of interest. Recent theoretical work has predicted that, when superconducting inclusions or boundaries are added to a phase-coherent normal sample, not only are well-known mesoscopic phenomena such as universal conductance fluctuations[1–3] (UCF's) changed in character, but also familiar properties of superconductors such as the Josephson effect[4–8] are fundamentally affected. In addition, novel interference effects, which couple to the order-parameter phase difference between multiple superconducting islands are predicted,[9–14] along with zero-bias anomalies arising from particle-hole symmetry breaking at finite energies.[15,16]

When analyzing problems in mesoscopic superconductivity, the question of self-consistency is rarely addressed. This arises in part from associated technical difficulties and in part from the fact that for many experiments such questions are of secondary interest. Consider, for example, an aluminum island embedded in a phase-coherent normal substrate such as silver. As the temperature or an applied magnetic field is decreased, the aluminum eventually undergoes a transition and in the region occupied by the island a superconducting order parameter $\Delta(\mathbf{r})$ switches on. In the region outside the island, due to the proximity effect, or, equivalently, Andreev scattering at the normal-superconductor interface, a pairing field $f(\mathbf{r}) = \langle \psi_\uparrow(\mathbf{r})\psi_\downarrow(\mathbf{r}) \rangle$ is induced, even though $\Delta(\mathbf{r})$ may be negligible there. Thus the aluminum is a source of the field $f(\mathbf{r})$ in much the same way that a nearby capacitor plate is a source of electric field. Provided one is not concerned with the properties of the aluminum, such as its critical field or temperature, questions of self-consistency are not of primary interest. Adopting the view that $\Delta(\mathbf{r})$ should be treated on the same footing as other experimentally accessible fields leads one naturally to ask how measurable quantities, such as the electrical conductance G of a phase-coherent normal host, are affected by the switching on of superconductivity. Recently Hui and Lambert[17,18] proved a simple theorem, which states that, when the normal-state conductance of a mesoscopic host is high enough, the introduction of superconductivity necessarily *decreases* the electrical conductance G. The main reason for highlighting this anomalous proximity effect (APE), which in clean systems is a consequence of the fact that G is bounded from above, is that it highlights the very different behavior of phase-coherent normal hosts, compared with their macroscopic counterparts, and motivates studies of dirty hosts, to which the theorem does not apply. For a superconducting order parameter of magnitude Δ_0, it was noted recently[17] that to lowest order the change in conductance δG arising from the switching on of a nonzero order parameter is of order Δ_0^2, and therefore the response coefficient $\chi_\Delta = \lim_{\Delta_0 \to 0} \partial G(\Delta_0)/\partial \Delta_0^2$ was introduced. This "Δ susceptibility" characterizes the change in G due to the onset of superconductivity and is independent of the magni-

tude of the superconducting order parameter. In Ref. 19 numerical results were presented which demonstrate that even dirty normal hosts can possess a negative χ_Δ. Furthermore, it was noted that χ_Δ scales with the system size and therefore conductance changes due to the onset of superconductivity may be many orders of magnitude greater than the quantum of conductance $2e^2/h$. At first sight, this is perhaps not surprising, because one intuitively expects the switching on of a superconducting order parameter to yield a gross increase in the conductance. However, we predict that χ_Δ can have arbitrary sign and therefore switching on superconductivity in a mesoscopic sample can produce a macroscopic *decrease* in conductance.

The aim of this paper is to present detailed theoretical predictions for the change δG. Experimentally, conductance anomalies near a superconducting transition[20–25] have recently been observed and we believe the analysis presented below and in Refs. 17 and 19 constitutes the first explanation of these APE's, based on a microscopic theory. An overview of the experimental situation will be presented in the discussion. In Sec. II, a method for computing G is outlined and in Sec. III, to highlight many of the qualitative properties of χ_Δ, numerical results for two-dimensional disordered systems are presented. The existence of large negative values of χ_Δ is not in itself sufficient to yield macroscopic negative changes in G, because the extent of the region over which G varies linearly with Δ_0^2 may be infinitesimal. In Sec. IV, to demonstrate that negative changes greater in magnitude than $2e^2/h$ do indeed occur, we examine δG at finite values of Δ_0 and show that the regime over which δG varies linearly with Δ_0^2 can extend to finite values of Δ_0. In Sec. V, we present analytic results for clean systems and examine the relationship between steps in the normal-state conductance and singularities in χ_Δ. In Sec. VI we examine the sensitivity of χ_Δ to the local environment of single atoms and demonstrate that for dirty systems single atomic changes can lead to fine structure in χ_Δ. Finally, in Sec. VII, the magnetic-field dependence of δG is computed and it is shown that the application of a field on the scale of a flux quantum through a sample both suppresses the magnitude and can change the sign of δG.

II. CALCULATION OF THE ZERO-TEMPERATURE Δ SUSCEPTIBILITY

For normal mesoscopic structures, smaller than the quasiparticle phase-breaking length, it is well known[26] that the precise value of the electrical conductance G depends on the nature of the normal leads, connecting the sample to external reservoirs. This situation persists in the presence of superconductivity and is therefore reflected in formulas for χ_Δ. In Ref. 27 it was shown that the Landauer formula[26] for the electrical conductance of a scatterer connected to two normal probes could be generalized to incorporate Andreev scattering and, more recently, generalizations of multiprobe formulas were obtained.[28] The two-probe result,[12,27,28] which has also been noted by Takane and Ebisawa,[29] contains the boundary conductance formula of Blonder, Tinkham, and Klapwijk[30] and the normal-state conductance[26] as limiting cases. In what follows, we examine the Δ susceptibility associated with the two-probe conductance only; multiprobe formulas can be obtained by applying the arguments which follow to the results of Ref. 28. Although the analysis can readily be generalized to finite temperatures, for simplicity we also restrict it to zero temperature.

The central quantity needed to compute transport properties of a phase-coherent sample possessing a Hamiltonian H and connected to external current-carrying leads is the quantum-mechanical scattering matrix $s(E,H)$, with submatrices $s^{\alpha,\beta}_{L,L'}(E,H)$ which describe the scattering of excitations of energy E from all incoming β channels of lead L' to all outgoing α channels of lead L (where $\alpha,\beta=+1$ for particles and -1 for holes). This satisfies unitarity and time-reversal symmetry, $s^{-1}(E,H)=s^\dagger(E,H)$ and $s(E,H^*)=s^t(E,H)$, while the submatrices satisfy the particle-hole symmetry relation

$$s^{\alpha,\beta}_{L,L'}(E,H)=\alpha\beta[s^{-\alpha,-\beta}_{L,L'}(-E,H)]^* .$$

From a knowledge of $s(E,H)$, a matrix of reflection and transmission coefficients can be constructed

$$P^{\alpha\beta}_{L,L'}(E)=\mathrm{Tr}\{s^{\alpha\beta}_{L,L'}(s^{\alpha\beta}_{L,L'})^\dagger\} ,$$

from which a variety of transport coefficients can be calculated. For example, the zero-temperature two-probe electrical conductance, in units of $2e^2/h$, is given by[27,28]

$$G=T_0+T_a+\frac{2(R_aR'_a-T_aT'_a)}{R_a+R'_a+T_a+T'_a} , \tag{1}$$

where we have noted that particle-hole symmetry at $E=0$ yields $P^{\alpha\beta}_{L,L'}(0)=P^{-\alpha,-\beta}_{L,L'}(0)$. The coefficients $R_0=P^{+,+}_{L,L}(0)$, $T_0=P^{+,+}_{L',L}(0)[R_a=P^{-,+}_{L,L}(0)$, $T_a=P^{-,+}_{L',L}(0)]$ are probabilities for normal (Andreev) reflection and transmission of quasiparticles from reservoir L, while R'_0,T'_0 (R'_a,T'_a) are corresponding probabilities for quasiparticles from reservoir L'. In the presence of N open channels per lead, these satisfy

$$R_0+T_0+R_a+T_a=R'_0+T'_0+R'_a+T'_a=N$$

and $T_0+T_a=T'_0+T'_a$.

Given the spatial form of the superconducting order parameter $\Delta(\mathbf{r})$ and the normal scattering potential $U(\mathbf{r})$, the scattering matrix can be computed by solving the Bogoliubov–de Gennes equation,

$$\begin{bmatrix} H_0 & \Delta \\ \Delta^* & -H_0^* \end{bmatrix}\begin{bmatrix}\psi(\mathbf{r})\\ \phi(\mathbf{r})\end{bmatrix}=E\begin{bmatrix}\psi(\mathbf{r})\\ \phi(\mathbf{r})\end{bmatrix} , \tag{2}$$

as outlined in Ref. 28. In what follows, we consider the situation in which the magnitude of the order parameter $\Delta(\mathbf{r})$ within the scatterer is characterized by a real, positive quantity Δ_0. Starting from Eq. (1), χ_Δ can then be obtained by differentiating with respect to Δ_0^2. In the case of a spatially symmetric sample, where coefficients associated with left- and right-going quasiparticles are identical, Eq. (1) reduces to

$$G = T_0 + R_a = N - (R_0 + T_a) , \tag{3}$$

in which case

$$\chi_\Delta = \lim_{\Delta_0 \to 0} \frac{\partial}{\partial \Delta_0^2}(T_0 + R_a) = - \lim_{\Delta_0 \to 0} \frac{\partial}{\partial \Delta_0^2}(R_0 + T_a) . \tag{4}$$

Since the limit $\Delta_0 \to 0$ is to be taken, $\Delta(\mathbf{r})$ can be treated perturbatively and all scattering coefficients computed using the "golden rules" for Andreev scattering introduced in Refs. 12 and 28. In Sec. V, this approach will be used to obtain analytic results for a clean, normal host in d dimensions, while in other sections results obtained by numerically solving Eq. (2) and differentiating Eq. (1) will be presented.

III. NUMERICAL RESULTS FOR χ_Δ IN TWO DIMENSIONS

In this section, we present the results of detailed numerical simulations of a two-dimensional tight-binding system, described by a Bogoliubov–de Gennes operator of the form

$$H = \begin{bmatrix} H_0 & \Delta \\ \Delta^* & -H_0^* \end{bmatrix} . \tag{5}$$

In this equation H_0 is a nearest-neighbor Anderson model on a square lattice, with off-diagonal hopping elements of value $-\gamma$, and Δ is a diagonal order-parameter matrix. The scattering region is chosen to be M sites wide and M' sites long and is connected to external leads of width M, as shown in Fig. 1. Within the scattering region, diagonal elements $\{\epsilon_i\}$ of H_0 are chosen to be random numbers, uniformly distributed between $\epsilon_0 - W$ and $\epsilon_0 + W$, while those of Δ are set equal to Δ_0. Within the leads, the diagonal elements of H_0 are equal to a constant ϵ_0, while those of Δ are set to zero. In what follows, for a given realization of the Hamiltonian H, the scattering matrix is obtained numerically, using a transfer matrix technique outlined in Appendix 2 of Ref. 28. The quantum-mechanical scattering states of energy E for such a system are functions of E/γ, Δ_0/γ, W/γ, $\{\epsilon_i/\gamma\}$, M, and M', although in what follows, for notational convenience, this full parametric dependence will not usually be shown explicitly.

Simulations of this model were reported in a recent Letter.[19] The results of Figs. 2–5 below both summarize and generalize those of Ref. 19. For these figures, $\gamma = 1$, all results are at zero energy, and, to avoid a discontinuity in the number of open channels at $E = 0$, the choice $\epsilon_0 = 0.09$ is made. To obtain results for a given width M, length M', and disorder W, a set of random diagonal elements $\{\epsilon_i\}$ of H_0 is generated. For each such set, the conductance $G(\Delta_0, M, M', W)$ is first obtained with $\Delta_0 = 0$, then recomputed with $\Delta_0 = 4 \times 10^{-4}$, and finally the derivative $\chi_\Delta(M, M', W)$ estimated from the difference between the two values. To aid comparison of results for systems with different widths, it is convenient to introduce the conductance per channel of the normal material,

$$\tilde{G}(0, M, M', W) = G(0, M, M', W)/N .$$

It should be noted that the quantity plotted in Figs. 2–8 of Ref. 19 is the susceptibility per open channel, $\tilde{\chi}_\Delta = \chi_\Delta / N$, not χ_Δ as stated in the figure captions therein. Figures 2 and 3 show results for a variety of M, M', and W, obtained by choosing a value of W, generating 500 sets of random diagonal elements, and computing the ensemble averages $\langle \tilde{\chi}_\Delta(M, M', W) \rangle$ and $\langle \tilde{G}(0, M, M', W) \rangle$, along with the rms deviations $\sigma_{\tilde{\chi}} = \langle [\tilde{\chi}_\Delta - \langle \tilde{\chi}_\Delta \rangle]^2 \rangle^{1/2}$ and

$$\sigma_{\tilde{G}} = \langle [\tilde{G}(0, M, M', W) - \langle \tilde{G}(0, M, M', W) \rangle]^2 \rangle^{1/2} .$$

To highlight the system-size dependence, Fig. 2 shows plots of $\langle \tilde{\chi}_\Delta(M, M', W) \rangle / M'^2$ versus $\langle \tilde{G}(0, M, M', W) \rangle$ for three values of M and three values of M', while Fig. 3 shows corresponding plots of $\sigma_{\tilde{\chi}}(M, M', W)/M'^2$. In view of the above-stated theorem in the zero-disorder limit, where $\tilde{G}(0) = 1$, one expects $\langle \tilde{\chi}_\Delta \rangle \leq 0$ and $\sigma_{\tilde{\chi}} = 0$. On the other hand, in the infinite-disorder limit, where both $\tilde{G}(0) = 0$ and $\tilde{G}(\Delta_0) = 0$, one expects $\langle \tilde{\chi}_\Delta \rangle = \sigma_\chi = 0$.[19] Between these two limits, $\langle \tilde{\chi}_\Delta \rangle$ passes through a maximum. Figure 2 indicates that for intermediate disorder, where $\langle \tilde{\chi}_\Delta \rangle$ varies linearly with $\langle \tilde{G}(0) \rangle$, the slopes of the graphs of $\langle \tilde{\chi}_\Delta \rangle M'^{-2}$ are independent of system size and therefore the total susceptibility χ_Δ is of the form

$$\chi_\Delta = N M'^2 \bar{\chi}_\Delta , \tag{6}$$

where

$$\langle \bar{\chi}_\Delta \rangle \simeq -B + C[1 - \langle \tilde{G}(0) \rangle] , \tag{7}$$

with B and C positive constants, independent of M and M'. The solid line drawn in Fig. 2 is a graph of $\langle \tilde{\chi}_\Delta \rangle M'^{-2}$ obtained from Eqs. (6) and (7), with $C = 6$ and $B = 0.5$.

Figure 3 suggests that for intermediate disorder plots of $\sigma_{\tilde{\chi}} M'^{-2}$ versus $\langle \tilde{G}(0) \rangle$ fall onto a single curve and therefore $\sigma_{\tilde{\chi}}$ is independent of the number of open channels N. The figure also shows that $\sigma_{\tilde{\chi}}$ vanishes at zero disorder and rises rapidly to a plateau region at intermediate disorder. In the latter region, which spans roughly the interval $0.99 < \langle \tilde{G}(0) \rangle < 0.5$, the fluctuations increase by only a factor of 2, whereas in the region $0.01 < \langle \tilde{G}(0) \rangle < 0.5$ they increase by an order of magnitude. At much larger values of disorder, where $G(0) \to 0$, both $\langle \tilde{\chi}_\Delta \rangle$ and the fluctuations vanish, as predicted by the ultrastrong-disorder analysis of Ref. 19. The width of $\tilde{G}(0)$ over which this occurs is extremely narrow and therefore these results would appear as a vertical column of points on the $G(0) = 0$ axis of Fig. 3. For clarity, we have chosen to omit these points from the figures.

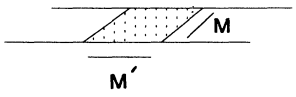

FIG. 1. Two-dimensional tight-binding system, of width M sites and length M' sites (shown shaded), connected to normal, crystalline, external leads of width M.

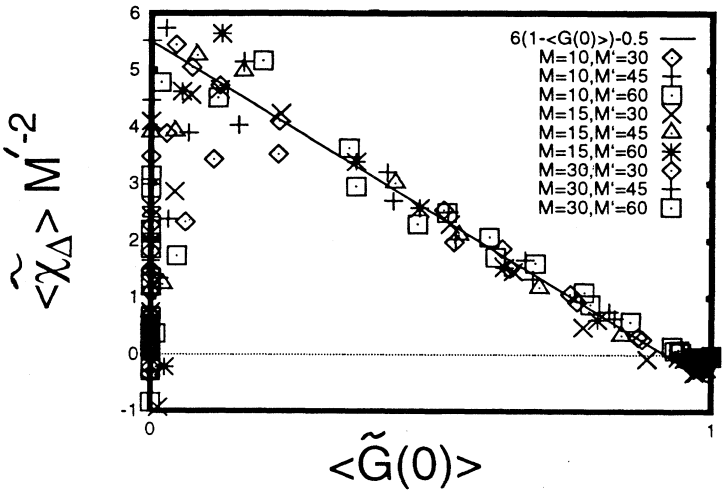

FIG. 2. Scaling curves of $\langle \tilde{\chi}_\Delta M'^{-2} \rangle$ for a variety of system sizes.

IV. RESULTS FOR THE FINITE Δ_0 CONDUCTANCE

Having summarized and expanded the results of Ref. 19, we now examine the magnitude of the conductance change $\delta G(\Delta_0)$, due to the switching on of a finite order parameter. In view of the scaling relation (6), we predict that for diffusive hosts χ_Δ scales with the number of open channels and therefore, as noted in Ref. 19, conductance changes due to the onset of superconductivity can in principle be much greater than $2e^2/h$. To demonstrate this convincingly, however, one must be sure that the region over which δG varies linearly with Δ_0^2 is finite. In Sec. V, we give examples of systems for which χ_Δ diverges, but with a linear region of infinitesimal width. In this section, results are presented which we believe are typical of homogeneously disordered systems in two dimensions. These demonstrate that, at least for weakly disordered structures, changes $\delta G(\Delta_0)$ of magnitude equal to many multiples of $2e^2/h$ and of arbitrary sign can indeed occur.

For four different values of disorder W, Fig. 4 shows results for $\delta\tilde{G}(\Delta_0)$ versus the ratio $\Delta_F=\Delta_0/E_F$, where $E_F=4\gamma-\epsilon_0$ is the Fermi energy. Results are shown for values of Δ_F up to $\Delta_F\sim 10^{-3}$, which is typical of a conventional superconductor. For each value of W, the figure shows results for several different realizations of the disorder. For the weaker disorders of $W=0.04$ and 0.4, Figs. 4(a) and 4(b), respectively, show that $\delta\tilde{G}$ is typically a monotonic function of Δ_0 and therefore the sign of χ_Δ yields the sign of $\delta\tilde{G}$ at finite Δ_0. For the larger disorders of $W=2.9$ and 3.9, corresponding to Figs. 4(c) and 4(d), respectively, if $\tilde{\chi}_\Delta$ is positive, $\delta\tilde{G}$ is typically monotonic. On the other hand, since the conductance is necessarily positive,

$$N>\delta G(\Delta_0)+G(0)>0\ , \tag{8}$$

and therefore if χ_Δ is negative the width $\delta\Delta_0$ of the linear regime must satisfy

$$\delta\Delta_0^2<G(0)/|\chi_\Delta|\ . \tag{9}$$

For large disorder, where $\tilde{G}(0)$ is typically small compared with unity, this condition can force $\delta\tilde{G}$ to vary nonlinearly, even for small values of Δ_F. In this case the

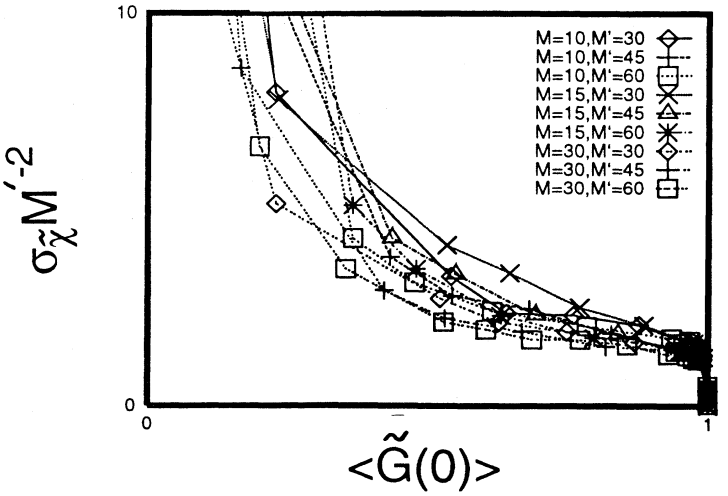

FIG. 3. Scaling curves of the standard deviation $\sigma_{\tilde{\chi}} M'^{-2}$.

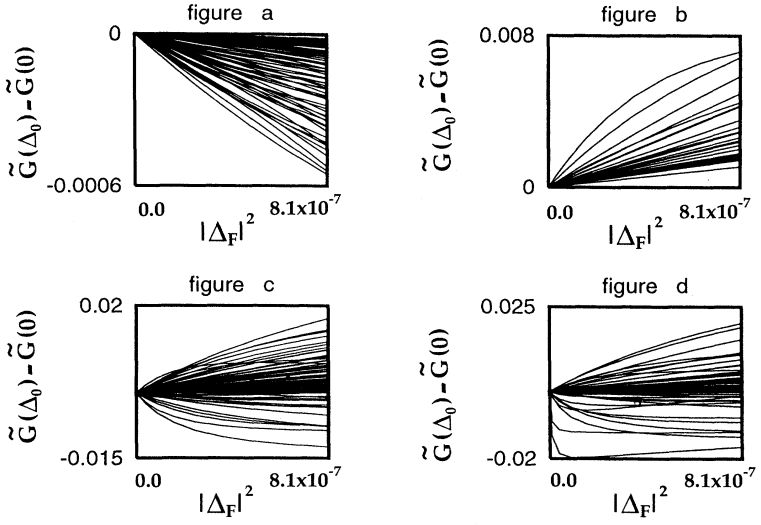

FIG. 4. For a system of size $M=M'=30$, this figure shows curves of the conductance per channel $\delta\tilde{G}$ versus the ratio $\Delta_F=\Delta_0/E_F$ for four values of the disorder width W, namely, $W=0.04$ (a), 0.4 (b), 2.9 (c), and 3.9 (d). For each value of W, results are shown for 50 different realizations of the site energies $\{\epsilon_i\}$. For these calculations $\gamma=1$, $\epsilon_0=0.09$, and $E=0$.

sign of χ_Δ still yields the most probable sign of δG for small but finite Δ_F. However, for much larger values, as would arise, for example, in a typical cuprate superconductor such as $YBa_2Cu_3O_{7-\delta}$, Fig. 5 illustrates that this is no longer the case. Figure 5 shows the large-disorder results from Fig. 4(d), plotted over a larger range of Δ_F, and demonstrates that by increasing Δ_F negative conductance changes can be made to change sign. For clarity only those results with a negative χ_Δ are plotted.

The above results demonstrate that the width of the liner regime is indeed finite and when combined with the scaling behavior (6) strongly suggest that the magnitude of APE's can increase with the number of open channels. Of course, ideally, one would like to see a more direct demonstration of this important feature. To obtain the total conductance change $\delta G=N\delta\tilde{G}$ from Figs. 4 and 5, one notes that, for a system of width $M=30$, with $\gamma=1$, $\epsilon_0=0.09$, $E=0$, the number of open channels is $N=27$. Therefore Figs. 4 and 5 show no example of systems for which δG is both negative and large compared with unity. Since the conductance $G(\Delta_0)$ is positive, to obtain examples of such conductance changes, it is of course necessary to simulate structures with a large normal-state conductance and therefore a large number of open channels. Computationally, the CPU time required to calculate the conductance of an $M\times M'$ system, using transfer matrix codes which reorthogonalize after each matrix multiplication, is proportional to M^3M' and systems with M greater than of order 10^2 are difficult to analyze. Therefore to demonstrate the existence of large negative values of δG we now focus attention on weakly disordered systems. Figure 6 shows results for a system of width $M=50$ and lengths $M'=20,50,100$ along with results for a system of width $M=100$ and length $M'=20$. In these calculations δG was computed using an order parameter of magnitude $\Delta_0=0.1$. For weak disorder, the system of width $M'=50$ yields negative values of δG of order 6, while for $M'=100$ δG is of order 11. These results clearly demonstrate the existence of large APE's, both for clean systems and in the presence of disorder. In the following section, where the zero-disorder limit is examined in more detail, we prove analytically that for clean systems this change scales with the system width.

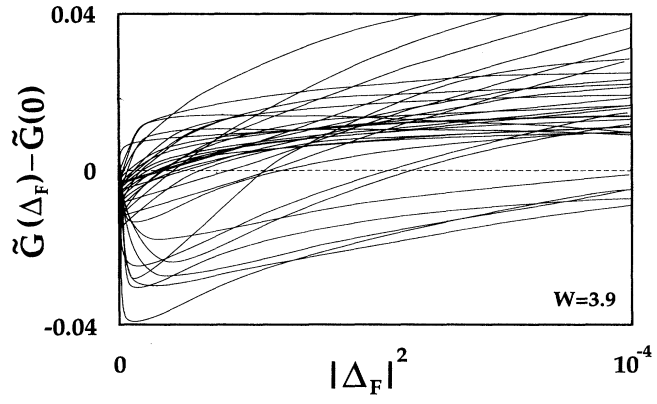

FIG. 5. As for Fig. 4(d), except that only results with a negative χ_Δ are shown and a larger range of Δ_F is used.

V. ANALYTICAL RESULTS FOR A CLEAN HOST

In this section, we obtain formulas for the Δ susceptibility of clean systems in one or more dimensions and for a long, clean system compute the change δG due to a finite Δ_0. As an example, consider a one-dimensional system with chemical potential μ, where

$$H_0(x)=-(\hbar^2/2m)\partial_x^2-\mu+U(x)\ ,$$

for which $U(x)$ and $\Delta(x)$ vanish outside the interval $0<x<L$. The scattering states of such a structure are obtained by noting, for example, that a solution of Eq. (2) corresponding to an incoming particle of energy E is of the form

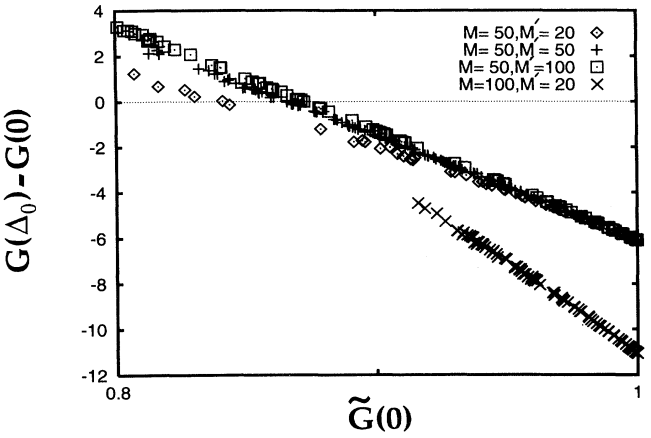

FIG. 6. Results for the total conductance change δG versus $\tilde{G}(0)$, for systems of size $M'=20$, $M=50$ (squares) and $M'=20$, $M=100$ (crosses). Each value corresponds to separate realizations of the site energies $\{\epsilon_i\}$. Since the disorder is weak, the fluctuations are small and therefore the results have not been ensemble averaged. For this calculation $\Delta_0=0.1$, $E=0$, $\gamma=1$, and $\epsilon_0=0.015$.

$$\begin{bmatrix}\psi(x)\\ \phi(x)\end{bmatrix}=\begin{bmatrix}\psi_0(x)\\ 0\end{bmatrix}+\int_0^L dx'\begin{bmatrix}G_+(x,x',E) & 0\\ 0 & G_-(x,x',E)\end{bmatrix}\times\begin{bmatrix}0 & \Delta(x')\\ \Delta^*(x') & 0\end{bmatrix}\begin{bmatrix}\psi(x)\\ \phi(x)\end{bmatrix}. \tag{10}$$

In this equation, $\psi_0(x)$ is an eigenstate of the normal host described by H_0, which for a unit incoming particle flux from the left is of the form

$$\psi_0(x)=v^{-1/2}\exp(ikx)+v^{-1/2}\int_0^L G_+(x,x',E)U(x')\exp(ikx)=v^{-1/2}\exp(ikx)+\psi_0^{\rm out}(x)\ , \tag{11}$$

where k is given by $\hbar^2k^2/2m=\mu+E$ and $v=\hbar k/m$ is the group velocity. The outgoing Green's functions of the normal host are given by

$$\begin{bmatrix}E-H_0(x) & 0\\ 0 & E+H_0^*(x)\end{bmatrix}\begin{bmatrix}G_+(x,x',E) & 0\\ 0 & G_-(x,x',E)\end{bmatrix}=\delta(x-x')\begin{bmatrix}1 & 0\\ 0 & 1\end{bmatrix} \tag{12}$$

and satisfy

$$G_\alpha(x,x',E)=-G^*_{-\alpha}(x,x',-E)\ .$$

In the limit $U(x)=0$, these reduce to the Green's functions for a clean host,

$$G_\alpha(x,x')=(i\hbar v)^{-1}\exp(i\alpha k|x-x'|)\ . \tag{13}$$

From Eq. (10), all reflection and transmission coefficients associated with an incident particle from the left can be written down by inspection. For example,

$$T_a=v|\phi(L)|^2=|t_a|^2=v\left|\int_0^L dx'G_-(L,x')\Delta^*(x')\psi(x')\right|^2 \tag{14}$$

and

$$R_a=v|\phi(0)|^2=|r_a|^2=v\left|\int_0^L dx'G_-(0,x')\Delta^*(x')\psi(x')\right|^2. \tag{15}$$

Similarly, if $\psi^{\rm out}(x)$ is the outgoing component of $\psi(x)$, then

$$R_0=v|\psi^{\rm out}(0)|^2=|r_0|^2=v\left|\psi_0^{\rm out}(0)+\int_0^L dx'G_+(0,x')\Delta(x')\phi(x')\right|^2=v\left|\psi_0^{\rm out}(0)+\int_0^L dx'dx''G_+(0,x')\Delta(x')G_-(x',x'')\Delta^*(x'')\psi(x'')\right|^2 \tag{16}$$

and

$$T_0=v|\psi(L)|^2=|t_0|^2=v\left|\psi_0(L)+\int_0^L dx'G_+(L,x')\Delta(x')\phi(x')\right|^2=v\left|\psi_0(L)+\int_0^L dx'dx''G_+(L,x')\Delta(x')G_-(x',x'')\Delta^*(x'')\psi(x'')\right|^2. \tag{17}$$

For the case where $\Delta(x)$ is equal to a constant Δ_0, in the interval $0<x<L$, replacing $\psi(x)$ by $\psi_0(x)$ on the right-hand sides of these expressions yields to order Δ_0^2

$$T_a=|\Delta_0|^2v\left|\int_0^L dx'G_-(L,x')\psi_0(x')\right|^2, \tag{18}$$

$$R_a=|\Delta_0|^2v\left|\int_0^L dx'G_-(0,x')\psi_0(x')\right|^2, \tag{19}$$

$$R_0=\bar{R}_0+|\Delta_0|^2 2v\ \mathrm{Re}\left[[\psi_0^{\mathrm{out}}(0)]^*\int_0^L dx'dx''G_+(0,x')G_-(x',x'')\psi_0(x'')\right], \tag{20}$$

and

$$T_0=\bar{T}_0+|\Delta_0|^2 2v\ \mathrm{Re}\left[[\psi_0(L)]^*\int_0^L dx'dx''G_+(L,x')G_-(x',x'')\psi_0(x'')\right], \tag{21}$$

where $\bar{R}_0$ and $\bar{T}_0$ are the reflection and transmission coefficients of the normal host. In what follows, we shall be interested in evaluating these formulas at zero energy, where k is replaced by $k_F=(2m\mu/\hbar^2)^{1/2}$ and v by $v_F=\hbar k_F/m$.

In more than one dimension, corresponding formulas for χ_Δ can be obtained from the multichannel golden rules written down in Ref. 12. By symmetry, expressions for coefficients arising from an incident particle from the right are obtained by substituting into the above expressions the Green's functions and wave functions corresponding to a normal potential $U(L-x)$. In general, if $U(x)=U(L-x)$ and $\Delta(x)=\Delta(L-x)$, then left-going and right-going coefficients are equal and Eqs. (3) and (4) can be used.

To obtain χ_Δ for a clean normal host, we first examine a clean one-dimensional system and then generalize the results to higher dimensions. For a clean embedding system of length L in one dimension, for which $U(x)=0$, $\psi_0(x)=v^{-1/2}\exp ikx$, Eq. (13) combines with expressions (19) and (21) to yield to order $|\Delta_0|^2$

$$R_a=\frac{|\Delta_0|^2L^2}{\hbar^2v_F^2} \tag{22}$$

and

$$T_0=1-\frac{|\Delta_0|^2L^2}{\hbar^2v_F^2}-\frac{|\Delta_0|^2\sin^2k_FL}{m^2v_F^4}\ . \tag{23}$$

These combine to yield

$$\chi_\Delta=\frac{-\sin^2k_FL}{m^2v_F^4}\ . \tag{24}$$

Before generalizing this to more than one dimension, it is interesting to note that a parallel analysis can be carried out for a tight-binding system of length $L=M'a$, described by a Hamiltonian of the form (5). In one dimension, the normal state possesses a dispersion relation of the form $E=\epsilon_0-2\gamma\cos ka$ and one finds that R_a, T_0, and χ_Δ are trivially obtained by replacing v_F and m in Eqs. (22)–(24) by their tight-binding counterparts

$$v_F=\frac{2\gamma a}{\hbar}\sin k_Fa \tag{25}$$

and

$$m=\frac{\hbar^2}{2\gamma a^2}\ . \tag{26}$$

In more than one dimension, since the system is translationally invariant in the transverse direction, each scattering state has a well-defined transverse momentum and a corresponding longitudinal wave vector k_n. In this case, the above approach is valid for each separate scattering channel n, provided v_F is replaced by the channel-dependent velocity v_n. Reflection and transmission coefficients, as well as χ_Δ, are then obtained by summing over all open channels, to yield

$$\chi_\Delta=\sum_{n=1}^{N}\frac{-\sin^2k_nL}{m^2v_n^4}\ . \tag{27}$$

This result is very general and can be applied to two or more dimensions.

For a continuum system, $v_n=\hbar k_n/m$, while for a two-dimensional tight-binding system, $v_n=(2\gamma a/\hbar)\sin k_na$. In the latter case, for a system of width M sites, with periodic boundary conditions in the transverse direction, the transverse wave vectors are $k_n^{(t)}=2\pi n/M$ and therefore the longitudinal wave vectors $k_n(E)$ of a quasiparticle of energy E are given by

$$E=\epsilon_0-4\gamma+4\gamma\sin^2k_n(E)a/2+4\gamma\sin^2\pi n/M\ . \tag{28}$$

For a given energy E, this yields N real, positive values for $k_n(E)$, which define the open channels of the system. From Eq. (27), the total zero-temperature susceptibility is

$$\chi_\Delta=\frac{-1}{4\gamma^2}\sum_{n=1}^{N}\frac{\sin^2k_n(0)L}{\sin^4k_n(0)a}\ . \tag{29}$$

The qualitative behavior of the right-hand side of Eq. (29) can be obtained by noting that the dominant contribution arises from the smallest denominator, which may be singly or doubly degenerate and which vanishes at normal-state conduction steps. Small denominators arise when the longitudinal velocity of one or more channels tends to zero and are therefore associated with quasiparticles incident at a grazing angle $\theta=\sin^{-1}(v_n/v_F)$. As an example, Fig. 7 shows the behavior of the normal-state

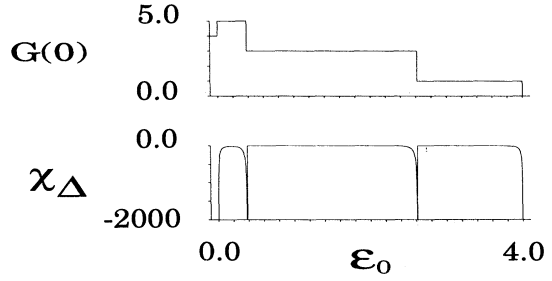

FIG. 7. The top figure shows the normal-state conductance $G(0)$ of a clean system as a function of the site energy ϵ_0. The lower figure shows that the corresponding χ_Δ is negative and diverges when steps occur in $G(0)$. For these calculations $\gamma=1$, $E=0$, and $M=M'=5$.

conductance $G(0)$ (upper graph) and χ_Δ as a function of ϵ_0. For this system, $M=M'=5$ and there are two doubly degenerate and one singly degenerate channels. Therefore $G(0)$ exhibits two conductance steps of magnitude 2 (in units of $2e^2/h$) and one step of height unity. At each of these steps, χ_Δ diverges. To quantify this behavior for systems of much larger width, let $\bar{n}$ be a value of n corresponding to the smallest denominator and let the degeneracy be $d_n(=1$ or 2). From (28), the value of the smallest denominator is

$$\sin^4 k_{\bar{n}}(0)a=[1-(\epsilon_0/2\gamma-\cos 2\pi\bar{n}/M)^2]^2$$

and therefore the value of ϵ_0 at which the nth channel closes is $\epsilon_n=\cos 2\pi n/M\pm 1$. To approximate χ_Δ in the interval $\epsilon_{\bar{n}-1}<\epsilon_0<\epsilon_{\bar{n}}$, where channel $\bar{n}-1$ is closed and channel $\bar{n}$ almost closed, it is convenient to expand ϵ_0 about $\epsilon_{\bar{n}-1}$. For small ϵ_0, $\bar{n}/(M/2)\simeq m$, where m is an integer, so writing $2\bar{n}=mM-l$, where $l/M\ll 1$, yields for the dominant contribution to the right-hand side of (29)

$$\chi_\Delta=\frac{-d_{\bar{n}}}{64\gamma^2}\frac{\sin^2 k_{\bar{n}}(0)L}{[\alpha/M^2-|\epsilon_0-\epsilon_{\bar{n}-1}|/4\gamma]^2} \tag{30}$$

with $\alpha=\pi^2|l|$. This shows that for small n/M χ_Δ is an oscillatory function of ϵ_0, bounded by an M-independent envelope. Furthermore, the M dependence of the denominator is removed by plotting χ_Δ/M^4 versus $\epsilon_0 M^2$, as shown in Fig. 8.

The physical origin of divergences in χ_Δ can be understood by examining curves of $G(\Delta_0)$ versus ϵ_0 for various values of Δ_0, shown in Fig. 9. For arbitrarily small but finite Δ_0, G becomes a continuous function of ϵ_0. Combining this with the theorem that χ_Δ is negative for clean systems guarantees the occurrence of divergent negative susceptibilities. It is important to note that the results shown in Fig. 9 lie outside a standard quasiclassical description of superconductivity, which at a clean normal-superconductor (N-S) interface insists that zero-energy excitations are Andreev reflected.[33] The curves shown in Fig. 9 are a result of competition between normal and Andreev scattering and for excitations incident at a grazing angle it is readily shown that normal scattering dominates. To emphasize this feature and to obtain an analytic result for the finite Δ_0 conductance change, we end this section by examining a long, clean N-S-N structure in more detail. Provided the superconductor is much longer than the superconducting coherence length $\xi=k_F^{-1}E_F/\Delta_0$, there is negligible quasiparticle transmission through the S region and therefore the total resistance reduces to the sum of two Blonder-Tinkham-Klapwijk (BTK) boundary resistances.[30] Since the boundaries are identical, this yields for the total conductance $G=R_a$ and since the system consists of decoupled channels R_a can be obtained by solving the Bogoliubov–de Gennes equation at a one-dimensional N-S interface. By insisting that scattered wave functions and their first derivatives be continuous at the boundary, one finds

$$R_a=\sum_{n=1}^{N} R_n\ , \tag{31}$$

where

$$R_n=\frac{2}{1+[1+(\Delta_0/\mu_n)^2]^{1/2}} \tag{32}$$

and $\mu_n=\hbar^2 k_n^2/2m$ is the longitudinal kinetic energy of a quasiparticle incident along channel n. Clearly, those channels corresponding to low-angle quasiparticles with $\mu_n<\Delta_0$ possess a small Andreev reflection probability R_n and, since there is no transmission, the corresponding normal reflection probability $(1-R_n)$ approaches unity. Finally, one obtains for the finite Δ conductance change due to the switching on of a uniform order parameter in a clean system

$$\delta G(\Delta_0)=\sum_{n=1}^{N}[R_n-1]=\sum_{n=1}^{N}\frac{1-[1+(\Delta_0/\mu_n)^2]^{1/2}}{1+[1+(\Delta_0/\mu_n)^2]^{1/2}}\ . \tag{33}$$

It should be noted that this result has been obtained in the limit of zero quasiparticle transmission and therefore Eq. (27) cannot be recovered by expanding Eq. (33) to order Δ_0^2. This is a reflection of the fact that the limits $L\to\infty$ and $\Delta_0\to 0$ do not commute. Indeed, the lowest-order contribution to Eq. (33) is obtained by replacing the numerator of Eq. (27) by -1, reflecting the fact that in the absence of quasiparticle transmission scattering processes from opposite ends of the superconductor do not interfere. It is interesting to note that, for both two- and three-dimensional structures, in the limit that the system width tends to infinity, the number of open channels with $\mu_n<\Delta_0$ is of order $N\Delta_0/\mu$. Hence Eq. (33) yields $\delta G(\Delta_0)/G(0)\simeq\Delta_0/\mu$, which demonstrates that δG scales with $G(0)$.

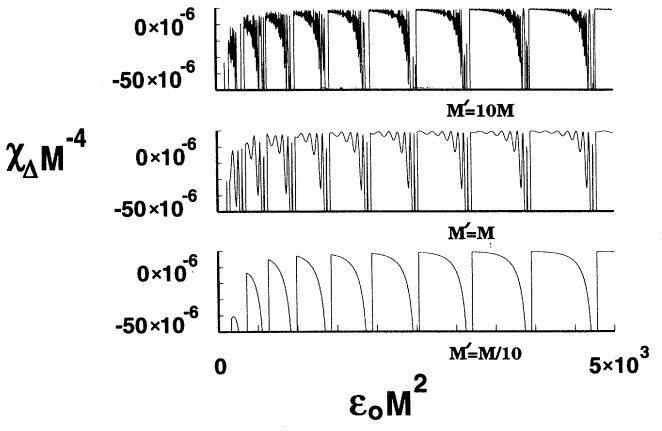

FIG. 8. This graph contains six plots of χ_Δ/M^4 $(=\tilde{\chi}_\Delta N/M^3)$ versus $\epsilon_0 M^2$, for $M=1000, 10\,000$ and $M'=M/10, M, 10M$, obtained from the exact result Eq. (29).

VI. THE ROLE OF RESONANCES

In this section we address a question begged by results of the form shown in Fig. 2(a), namely, why do systems

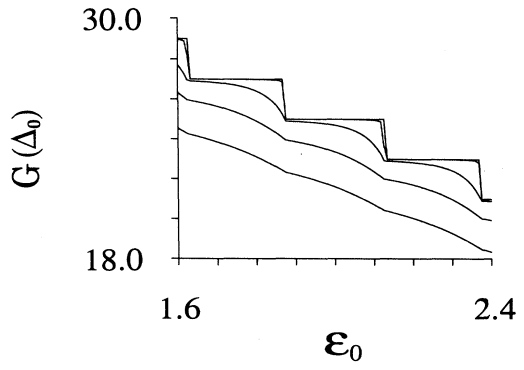

FIG. 9. Curves of the total conductance $G(\Delta_0)$ versus ϵ_0 for five values of Δ_0 and a system of size $M=50$, $M'=5$. The upper curve corresponds to $\Delta_0=10^{-4}$, the next three curves to $\Delta_0=10^{-2}$, $\Delta_0=0.1$, and $\Delta_0=0.3$, and the bottom curve to $\Delta_0=0.5$.

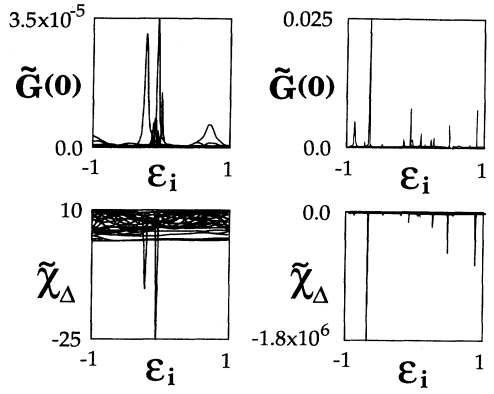

FIG. 10. For $M=10$, $M'=20$, and a disorder of $W=6$, the left-hand pair of figures show results obtained by successively varying the site energies ϵ_i of the 50 leftmost sites. The right-hand pair show results for the next 50 sites. The upper pair of graphs show results for the normal-state conductance and the bottom pair of graphs show results for the corresponding values of $\tilde{\chi}_\Delta$. For these calculations, $\gamma=1$ and $\epsilon_0=0.2$. The latter value is chosen such that the system is half way between discontinuities in the normal-state conductance.

with the same normal conductance possess markedly different susceptibilities? The results of the previous section go part way towards answering this question, since they reveal that χ_Δ is sensitive to fine-scale structure in the normal-state conductance. For clean systems this structure takes the form of well-known conductance steps. For strongly disordered systems, it is known[31,32] that $G(0)$ can exhibit sharp resonances and in this section we examine the role of such features.

Resonances in $G(0)$ can be obtained both by varying the scattering potential at constant energy and by varying the quasiparticle energy for a fixed scattering potential. Experimentally, resonances in $G(0)$ reveal themselves through the motion of two-level systems, which can cause observable changes in $G(0)$.[31] For this reason, rather than focus attention on the energy dependence of $G(0)$ and χ_Δ, we examine the sensitivity of these quantities to the adiabatic motion of single atoms, which is modeled by varying the diagonal elements ϵ_i of individual sites. To this end, consider a rectangular scattering region of width M and length M', containing $M\times M'$ sites. Let the labels attached to the diagonal elements of the leftmost column of sites be $i=1,2,\ldots,M$, those belonging to the next column $i=M+1,M+2,\ldots,2M$, and so on. For a given realization of the random elements $\{\epsilon_i\}$, we select a particular site j and vary ϵ_j between the limits $-\gamma$ and $+\gamma$. After plotting $G(0)$ versus ϵ_j, the latter is returned to its original (random) value and the whole exercise repeated for the next value of j. For $M=10$ and $M'=20$, the left-hand plots of Fig. 10 show results for the 25% of sites $1\le j\le MM'/4$ nearest the left end of the scattering region, while the right-hand plots show results for sites $MM'/4+1\le j\le MM'/2$, which are closer to the center of the scatterer. These results were obtained with a rather large disorder, $W=6$. Figure 11 shows corresponding results for a smaller disorder, $W=4$. The upper pairs of graphs in these figures show results for the normal-state conductance per channel, while the bottom pairs show the corresponding values for $\tilde{\chi}_\Delta$. Sites located near the center of the scatterer yielded larger and more narrow resonances than their counterparts near the boundaries, as predicted by a Breit-Wigner formula for normal transmission resonances.[32] As noted above, such resonances reveal themselves experimentally through the motion of single defects and therefore Figs. 10 and 11 predict that the corresponding Δ susceptibility should also be sensitive to such motion.

VII. BEHAVIOR OF $\tilde{\chi}_\Delta$ IN A MAGNETIC FIELD

Having analyzed the zero-field behavior of $\tilde{\chi}_\Delta$, we now examine the effect of switching on a weak magnetic field in a direction normal to the plane of the sample. The aim of this calculation is to highlight the generic response of χ_Δ to an applied magnetic field and therefore, as noted in paragraph 2 of the Introduction, self-consistency is not of primary interest. Nevertheless, any model employed

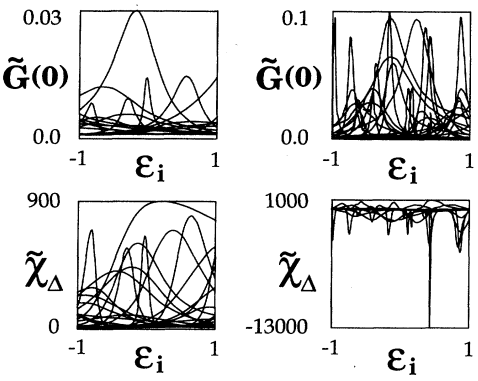

FIG. 11. As for Fig. 10, but with $W=4$.

must at least contain the qualitative features expected of a self-consistent solution. In what follows, we consider a type-II superconductor of size L greater than or of the order of the coherence length ξ, but much less than the magnetic penetration length λ. In this case the applied field is not excluded and, since it costs condensation energy to create a vortex, a weak field is expected to have a negligible effect on both the phase and the magnitude of the order parameter. Indeed, textbook solutions[34] for the order parameter in a thin film of thickness L less than or of the order of a critical thickness $L_c \simeq 1.8\xi$ show that the phase of the order parameter is unchanged by the application of fields equivalent to many flux quanta through the sample. Since we are only interested in the response of χ_Δ to fields of the order of a flux quantum through the sample, any changes in the order parameter will be assumed negligible and the field applied via a Peierls substitution, by introducing appropriate phase factors into the off-diagonal elements of H_0.

The left-hand graph of Fig. 12 shows plots of $\langle \tilde{\chi}_\Delta \rangle$ versus the flux ϕ passing through the sample, in units of the flux quantum $\phi_0 = hc/e$. The right-hand graph shows corresponding results for the fluctuations. In these simulations, the scatterer is chosen to be a square of size $M = M' = 20$ sites, with periodic boundary conditions and $N = 17$ open channels. For each of ten disorders W, 500 sets of random diagonal elements ϵ_i are generated. For each of the 500 samples, the $\tilde{G}(0)$ and $\tilde{\chi}_\Delta$ are computed for ten different values of magnetic flux.

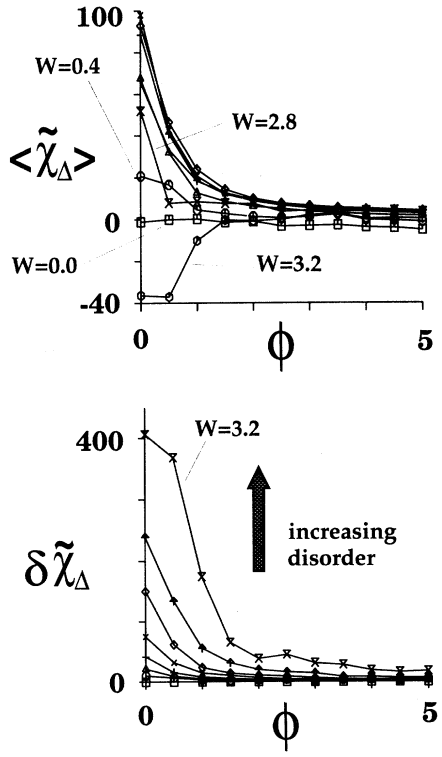

FIG. 12. Graphs of the ensemble averages $\langle \tilde{\chi}_\Delta \rangle$ (upper) and $\langle \delta\tilde{\chi}_\Delta \rangle$ (lower), plotted against the flux ϕ through the sample, in units of the flux quantum hc/e. For these calculations, $M = M' = 20$, $\gamma = 1$, and $\epsilon_0 = 0.2$. Results are shown for seven equally spaced values of disorder, ranging from $W = 0$ to 3.2.

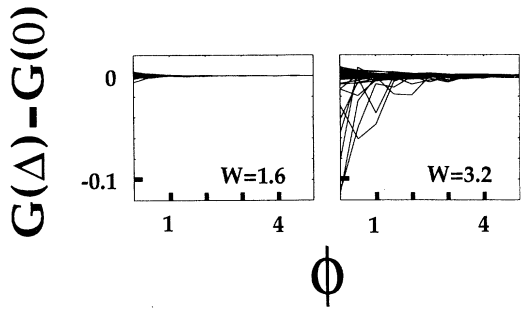

FIG. 13. For $W = 1.6$ (left graphs) and $W = 3.2$ (right graphs), this figure shows the flux dependence of the finite Δ conductance change for a 20×20 system, with a uniform order parameter of magnitude $\Delta = 0.001$. In these calculations, $\gamma = 1$ and $\epsilon_0 = 0.2$.

In all cases, one finds that the magnitude of both $\langle \tilde{\chi}_\Delta \rangle$ and $\langle \delta\tilde{\chi}_\Delta \rangle$ is suppressed when ϕ is of order unity and therefore the typical size of a conductance change due to the onset of superconductivity is diminished. For two values of the disorder, Fig. 13 shows an example of the flux dependence of the finite Δ conductance change of individual samples and reveals that changes in the sign of $\delta\tilde{G}$ can occur, when ϕ varies on the scale of ϕ_0. Consequently, the probability P_- of finding a negative value for χ_Δ is expected to be field sensitive. This feature is illustrated in Fig. 14, which shows plots of P_- versus ϕ.

VIII. DISCUSSION

In this paper, we have presented analytical results for clean systems and numerical results for disordered sys-

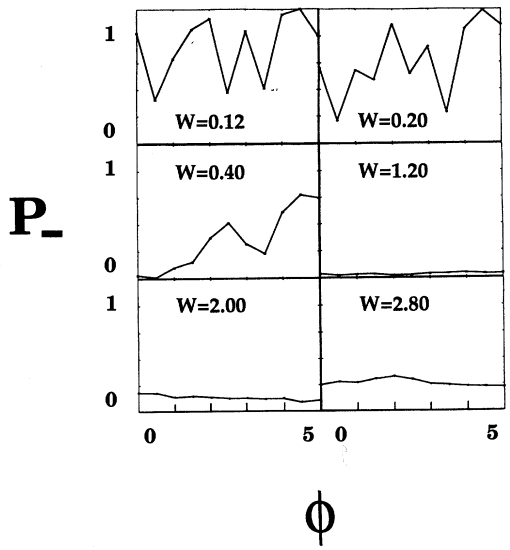

FIG. 14. For six values of disorder ranging from $W = 0.12$ to 2.8, this figure shows how the probability P_- of obtaining a negative value of χ_Δ changes with the applied magnetic flux ϕ. For these calculations, $M = M' = 20$, $\gamma = 1$, and $\epsilon_0 = 0.2$.

tems, which describe the effect of a superconducting order parameter on a phase-coherent normal host. Using a microscopic description based on exact solutions of the Bogoliubov–de Gennes equation, we have demonstrated that the onset of superconductivity can be accompanied by gross *negative* changes in the electrical conductance. From results such as those contained in Fig. 2(a) we predict that negative conductance changes are likely to occur for either dirty or clean systems, although for intermediate disorders the average conductance change is positive. Both the susceptibility χ_Δ and the conductance change δG at finite Δ_0 have been examined. Figure 4 shows that for homogeneously disordered systems, with $\Delta_0/E_F \ll 1$, the sign of χ_Δ is typically a reliable guide to the sign of δG over a finite region of Δ_0. However, if the ratio Δ_0/E_F is increased to larger values, typical of cuprate superconductors, δG can change sign. Analytical results for clean systems predict that χ_Δ diverges at normal-state conductance steps. This behavior is a reflection of the fact that superconductivity suppresses conductance steps and shifts plots such as $G \rightarrow \epsilon_0$ to lower values of G, as predicted by a recent theorem.[17,19] Since normal-state conductance steps are observable experimentally, this should be a striking property of clean mesoscopic structures. In dirty structures, where two-level systems can lead to observable changes in the normal-state conductance, we predict that measurable changes in χ_Δ and δG will also occur. Finally, in Sec. VII, we predict that a magnetic field on the scale of a flux quantum through the sample will suppress the magnitude of χ_Δ. It should be emphasized that the results presented in this paper are based on exact solutions of the Bogoliubov–de Gennes equation and therefore go beyond standard quasiclassical approaches to superconductivity. This is necessary, because quasiclassical theory does not contain known mesoscopic phenomena such as the transport resonances of Sec. VI. Nor does it correctly describe low-angle, normal scattering at clean interfaces as outlined in Sec. V.

During the past three years, there have been a number of experiments reporting resistance anomalies due to the onset of superconductivity in phase-coherent structures. These can be divided into two classes; those such as Refs. 22, 23, and 35, for which the external leads are normal, and those such as Refs. 20, 21, 24, and 25, which have superconducting external leads. The former yields a zero-temperature conductance change δG with a sample-dependent sign, whose magnitude can be many times larger than $2e^2/h$ and which (see, e.g., Fig. 3 of Ref. 34) is diminished by the application of a weak magnetic field, in broad agreement with our predictions. It should be noted that, while we have computed χ_Δ by switching on a uniform order parameter, the calculations reported here could easily be repeated for small superconducting islands embedded in the arms of phase-coherent normal loops, as in Refs. 22 and 23. The effect reported here is a generic phenomenon and arises even if $\Delta(\mathbf{r})$ is nonzero over only a portion of the scatterer. It does not require that a finite $\Delta(\mathbf{r})$ be induced in the normal host via the proximity effect. The only requirement is that Andreev scattering takes place at the interface and therefore $f(\mathbf{r})$ is nonzero in the host material.

In contrast to the anomaly of Refs. 22 and 23, which persists to the lowest available temperature, the experiments of Refs. 20, 21, 24, and 25 yield a conductance anomaly near T_c which vanishes at low temperatures. This occurs because the external probes become superconducting at temperature $T_p < T_c$, thereby destroying the measurement. Vaglio *et al.*[36] have cautioned that anomalies of this kind can arise through inhomogeneities in the system and may have no direct relevance to mesoscopic superconductivity. Nevertheless, for structures which are phase coherent in the interval $T_p < T < T_c$, the theory outlined above should apply. Interestingly, the experiments of Ref. 25 reveal that a magnetic field suppresses the conductance anomaly, in agreement with our theoretical predictions. However, sample-to-sample fluctuations in the sign of δG have not been reported.

ACKNOWLEDGMENTS

This work is supported by the SERC, the EC SCIENCE program, and the MOD. It has benefited from useful conversations with M. Leadbeater and V. Petrashov.

[1]Y. Takane and H. Ebisawa, J. Phys. Soc. Jpn. **60**, 3130 (1991).
[2]R. A. Jalabert, J.-L. Pichard, and C. W. J. Beenakker, Phys. Rev. B **48**, 2811 (1993).
[3]J. T. Bruun, V. C. Hui, and C. J. Lambert, Physica B **194-196**, 1623 (1994).
[4]L. I. Glazman and K. A. Matveev, JETP Lett. **49**, 659 (1989).
[5]C. W. J. Beenakker and H. van Houten, Phys. Rev. Lett. **66**, 3056 (1991).
[6]A. Furusaki, H. Takayanagi, and M. Tsukada, Phys. Rev. Lett. **67**, 132 (1991).
[7]P. F. Bagwell, Phys. Rev. B **46**, 12 573 (1992).
[8]C. J. Lambert and A. Martin, J. Phys. Condens. Matter **6**, L221 (1994).
[9]B. Z. Spivak and D. E. Khmel'nitskii, JETP Lett. **35**, 413 (1982).
[10]H. Nakano and H. Takayanagi, Solid State Commun. **80**, 997 (1991).
[11]S. Takagi, Solid State Commun. **81**, 579 (1992).
[12]C. J. Lambert, J. Phys. Condens. Matter **5**, 707 (1993).
[13]V. C. Hui and C. J. Lambert, Europhys. Lett. **23**, 203 (1993).
[14]F. W. Hekking and Yu. Nazarov, Phys. Rev. B **49**, 6847 (1994).
[15]A. F. Volkov, A. V. Zaitsev, and T. M. Klapwijk, Physica C **210**, 217 (1993).
[16]I. K. Marmakos, C. W. J. Beenakker, and R. A. Jalabert, Phys. Rev. B **48**, 2811 (1993).
[17]V. C. Hui and C. J. Lambert, Physica B **194-196**, 1673 (1994).
[18]It should be noted that several terms are missing from Eq. (4) of Ref. 17, all of which vanish in the limit $\Delta_0 \rightarrow 0$ and therefore do not affect the validity of the theorem. This typographical error is repeated in Eq. (4) of Ref. 19.
[19]V. C. Hui and C. J. Lambert, J. Phys. Condens. Matter **5**,

L651 (1993).
[20]Y. W. Kwong, K. Lin, P. J. Hakonen, M. S. Isaacson, and J. M. Parpia, Phys. Rev. B **44**, 462 (1991).
[21]P. Santhanam, C. C. Chi, S. J. Wind, M. J. Brady, and J. J. Bucchignano, Phys. Rev. Lett. **66**, 2254 (1991).
[22]V. T. Petrashov and V. N. Antonov, JETP Lett. **54**, 241 (1991).
[23]V. T. Petrashov, V. N. Antonov, S. V. Maksimov, and R. Sh. Shaikhaidarov, JETP Lett. **58**, 49 (1993).
[24]J.-J. Kim, J. Kim, S. Lee, H. J. Lee, K. W. Park, H. J. Shin, and E.-H. Lee, Physica B **194-196**, 1035 (1994).
[25]J.-J. Kim, J. Kim, S. Lee, H. J. Lee, K. W. Park, H. J. Shin, and E.-H. Lee (unpublished).
[26]For a discussion of various formulas applicable to normal systems, see M. Büttiker, IBM J. Res. Dev. **32**, 317 (1988).
[27]C. J. Lambert, J. Phys. Condens. Matter **3**, 6579 (1991).
[28]C. J. Lambert, V. C. Hui, and S. J. Robinson, J. Phys. Condens. Matter **5**, 4187 (1993).
[29]Y. Takane and H. Ebisawa, J. Phys. Soc. Jpn. **61**, 1685 (1992).
[30]G. E. Blonder, M. Tinkham, and T. M. Klapwijk, Phys. Rev. B **25**, 4515 (1982).
[31]G. A. Garfunkel, G. B. Alers, and M. B. Weissman, Phys. Rev. B **41**, 4901 (1990).
[32]M. Büttiker, IBM J. Res. Dev. **32**, 63 (1988).
[33]J. W. Serene and D. Rainer, Phys. Rep. **101**, 221 (1983).
[34]W. Tinkham, *Introduction to Superconductivity* (McGraw-Hill, New York, 1975).
[35]V. T. Petrashov, V. N. Antanov, and M. Persson, Phys. Scr. **T42**, 136 (1992).
[36]R. Vaglio, C. Attanasio, L. Maritato, and A. Ruosi, Phys. Rev. B **47**, 15 302 (1993).